Published in Biosensors and Bioelectronics 21, issue 1, 167-174, 2005
which should be used for any reference to this work

High-density electrode array for imaging in vitro electrophysiological activity

L. Berdondini[a,*], P.D. van der Wal[a], O. Guenat[a], N.F. de Rooij[a], M. Koudelka-Hep[a], P. Seitz[b], R. Kaufmann[b], P. Metzler[b], N. Blanc[b], S. Rohr[c]

[a] *Sensors, Actuators and Microsystems Laboratory, Institute of Microtechnology, University of Neuchâtel, Rue Jaquet-Droz 1, CH-2007 Neuchâtel, Switzerland*
[b] *Image Sensing Section, Centre Suisse d'Electronique et Microtechnique (CSEM SA), Badenerstrasse 569, 8048 Zürich, Switzerland*
[c] *Physiologisches Institut, University of Bern, Bühlplatz 5, 3012 Bern, Switzerland*

Abstract

The development of a high-density active microelectrode array for in vitro electrophysiology is reported. Based on the Active Pixel Sensor (APS) concept, the array integrates 4096 gold microelectrodes (electrode separation 20 μm) on a surface of 2.5 mm × 2.5 mm as well as a high-speed random addressing logic allowing the sequential selection of the measuring pixels. Following the electrical characterization in a phosphate solution, the functional evaluation has been carried out by recording the spontaneous electrical activity of neonatal rat cardiomyocytes. Signals with amplitudes from 130 $\mu V_{p\text{-}p}$ to 300 $\mu V_{p\text{-}p}$ could be recorded from different pixels. The results demonstrate the suitability of the APS concept for developing a new generation of high-resolution extracellular recording devices for in vitro electrophysiology.

Keywords: Microelectrode array; High-density; APS–MEA; Electrophysiology; In vitro

1. Introduction

The recordings of extracellular potentials from cultured excitable cells using microelectrode arrays (MEAs) have become a well-accepted technique in both fundamental research and applied electrophysiology. At present, multi-site recordings aimed at monitoring distributed patterns of electrical activities of neuronal or cardiomyocyte cell cultures are exploited in the investigation of signal propagation and processing, learning processes and memory (DeMarse et al., 2001; Jimbo et al., 1999; Mussa-Ivaldi and Miller, 2003; Shahaf and Marom, 2001). Furthermore, the MEAs serve as test-platforms for toxicological studies, drug screening and cell-based biosensors (DeBusschere and Kovacs, 2001; Keefer et al., 2001; Morefield et al., 2000; Offenhäusser and Knoll, 2001).

The current MEAs (Gross et al., 1982; Pine, 1980) provide typically 30–160 electrodes with inter-electrode spacing of 100–500 μm. Several MEAs are already commercially available (Multichannel Systems; Panasonic; Ayanda-Biosystems). These arrays are fabricated mainly by thin-film technology with Pt, Au, IrO_x, ITO and TiN microelectrodes embedded in an insulation layer of Si_3N_4, EPON SU-8 or polyamide. The cells are plated and cultured directly on the active area allowing the non-invasive, long-term (up to several months) monitoring and stimulation of the network electrophysiological activity.

Because the recorded signals originate from the cells in close proximity to the electrodes and because of the random distribution of the cellular networks, the number of recording sites, i.e., the spatial resolution, is therefore limited. Considering a typical culture of 50,000 neurons and typically 50 electrodes, this represents an under-sampling of the network activity by a factor 1000. Although the number of electrodes could be increased on the same thin-film technological basis, there are practical limits imposed by the manageable num-

* Corresponding author. Tel.: +41 32 720 55 20; fax: +41 32 720 57 11.
E-mail address: luca.berdondini@unine.ch (L. Berdondini).

ber of electrode-contact pad connections and by the rising complexity of the external amplification circuit.

There are four approaches that are pursued in order to increase the number of effective recording sites. The first one consists of patterning the cell networks on MEAs by using adhesion promoters/inhibitors or guiding microstructures (Heiduschka et al., 2001; Martinoia et al., 1999; Saneinejad and Shoichet, 2000; Yeung et al., 2001). The second methodology relies on confinement of individual neurons over each electrode, the so-called neuro-cages, built in a way allowing the formation of networks (Maher et al., 1999). In the third approach, a large number of closely spaced electrodes are addressed by a methodology based on light-addressable potentiometric sensors (LAPS) (George et al., 2000a,b). LAPS-based MEAs integrate thousands of microelectrodes addressed by a laser. Thus, Bucher et al. (2001) describe a light-addressable microelectrode chip with 3600 electrodes on a surface of 1.8 mm $\times$ 1.8 mm. Although the number of electrodes can be dramatically increased using LAPS, the issues of lateral resolution, speed of addressing and possible phototoxic effects during long-term recordings still remain to be assessed (George et al., 2000a,b).

A further concept, based on standard complementary metal-oxide-semiconductor (CMOS) technology, seems particularly attractive for overcoming the current spatio-temporal limitations. The CMOS design allows fabrication of high-density structures, on-chip amplification and integration of additional electronic circuitry to be realized by a commercially available process. CMOS circuits developed for in vivo or for in vitro recording with MEAs have been reported previously, in particular as off-chip or on-chip amplification circuits (Bai and Wise, 2001; Najafi and Wise, 1986; Pancrazio et al., 1998), for multi-parametric devices (Lehmann et al., 2001) or for portable biosensor systems (DeBusschere and Kovacs, 2001). More recently, CMOS arrays featuring 4 $\times$ 4 metallic electrodes with a pitch of 250 μm and on-chip amplification and stimulation circuits (Heer et al., 2004) as well as a high-density FET array with non-metallized gates (Eversmann et al., 2003) have been reported.

The aim of our work is to develop high-density metallic microelectrode arrays for a high spatio-temporal resolution imaging of the electrophysiological activity of electrogenic cell cultures. To achieve this, considering the potential advantages of metallic electrodes for low-noise recordings, we have adopted a different CMOS design (Fig. 1), namely a solid-state active pixel sensor (APS) concept that was originally developed for image sensors (Willemin et al., 2001). Realized by CMOS technology, the APS allows, upon modifying the pixels' functionality, a straightforward integration of metallic microelectrodes, on-chip and in-pixel amplification, timing and control circuits and multi-plexers (Berdondini et al., 2002, 2003).

Here, we report on the development of an APS-based high-density MEA (APS–MEA). It consists of an array of 64 $\times$ 64 pixel elements on an overall active area of 2.5 mm $\times$ 2.5 mm. Each pixel defines a surface of 40 μm $\times$ 40 μm and comprises

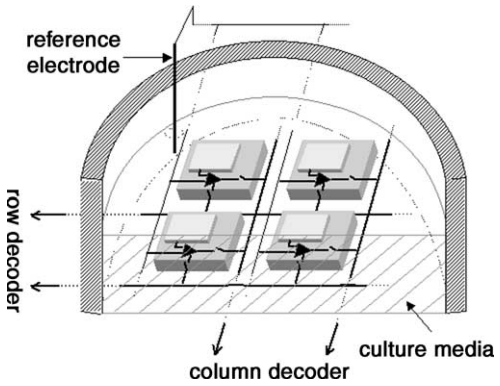

Fig. 1. The APS–MEA concept.

a gold microelectrode of 20 μm $\times$ 20 μm and an underneath pre-amplifier. The same addressing logic circuit, previously developed for light-sensitive APS devices, has been implemented in this first-generation of APS–MEAs. The addressing logic is integrated on the sides of the chip and allows the sequential addressing of all pixels or of a pre-defined sub-set at a maximum sampling frequency of 10 MHz.

The design parameters, electrical characterizations and multi-pixel recordings of the spontaneous activity of neonatal rat cardiomyocyte cultures are presented.

2. Materials and methods

2.1. System design

The device was designed on Mentor Graphics (Mentor Graphics Corporation, Wilsonville, USA), and fabricated using a standard 0.5 μm CMOS technology (Alcatel Microelectronics, 5 metal layers technology).

The addressing logic of an existing APS system was adapted to the 64 $\times$ 64 pixel array, and the pixel circuit was designed for electrophysiological recordings. The same in-pixel circuit was integrated in all the 4096 pixels, and the microelectrodes were designed as contact pads measuring 20 μm $\times$ 20 μm.

2.2. Design of the in-pixel pre-amplifier

The in-pixel pre-amplifier has to fit into the pixel dimensions, and thus only circuits with low number of transistors were considered. We opted for a differential amplifier, the five transistor operational transconductance amplifier (5-OTA), because of its high open-gain and stability to bias voltages when operated in common-mode (Fig. 2A). It amplifies both continuous (DC) and alternating (AC) signals applied on the differential pair, constituted of the n-MOS transistors MN1 and MN2. The p-MOS transistors MP1 and MP2 and the n-MOS transistors MN3 and MN5 form two current mirrors.

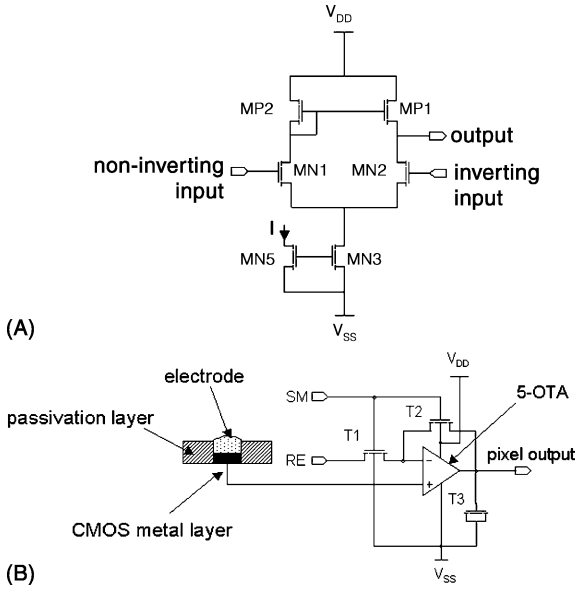

Fig. 2. (A) Schematic of the 5-OTA (B). Schematic of the in-pixel pre-amplifier.

The transistors of the pre-amplifier were optimised by simulations on Accusim (Mentor Graphics Corporation, Wilsonville, USA) in order to achieve the highest open-loop gain and the lowest noise. Analytically, considering the model of strong inversion of a MOS transistor, it can be found that (i) the gain increases by the square root of the gate width of the input transistors (MN1, 2); (ii) the gain increases when the gates of the transistors in the current mirror (MP1, 2) are longer than in the differential pair (MN1, 2); and that (iii) the gain increases by the square root of decreasing drain-source current.

The noise was reduced by design optimisation simulating the contributions of thermal noise, shot noise and flicker noise (1/*f* noise) and calculating the referred input noise as the sum of the noise sources referred to the input transistors. Noise is reduced with wide gates in the differential pair by increasing the transistor transconductances and with long gates in the transistors of the current mirror by decreasing their transconductances.

In addition to the five transistor operational transconductance amplifier (5-OTA), in each pixel three additional transistors (T_1, T_2 and T_3) were integrated as can be seen in Fig. 2B. This allows operating the pre-amplifier in open or closed-loop modes. In the open-loop mode the signal is directly amplified by the open-gain, while in the closed-loop mode the gain is set to one and the pre-amplifier acts as an impedance transformer. Transistors T_1 (n-MOS) and T_2 (p-MOS) function as voltage controlled switches. Applying V_{SS} (0 V) or V_{DD} (3.3 V) on their gates (SM), it is possible to select the closed-loop configuration ($T_1 \rightarrow \infty$ and $T_2 \rightarrow 0$) or the open-loop configuration ($T_1 \rightarrow 0$ and $T_2 \rightarrow \infty$), respectively. The SM voltage and the reference electrode (RE) are common to all pixels.

In the open-loop mode, while the non-inverting input of the pre-amplifier is connected to the pixel microelectrode, the reference electrode, which is common to all microelectrodes, is externally connected to the inverting input (Fig. 3A). The DC polarization on both inputs ($V_{DC,\,in}$) control the open-loop gain and bandwidth.

In the closed-loop mode, the reference electrode is not connected (Fig. 3B). The amplifier has a gain of one and acts as an impedance transformer. Transistor T_3 is a MOS output capacitance characterized by a 10 μm $\times$ 10 μm gate surface and with a value of 400 fF. It is used for lowering the output signal bandwidth.

The single pixel layout is shown in Fig. 4. Transistor MN5 is common to all microelectrodes and it is integrated outside the pixels.

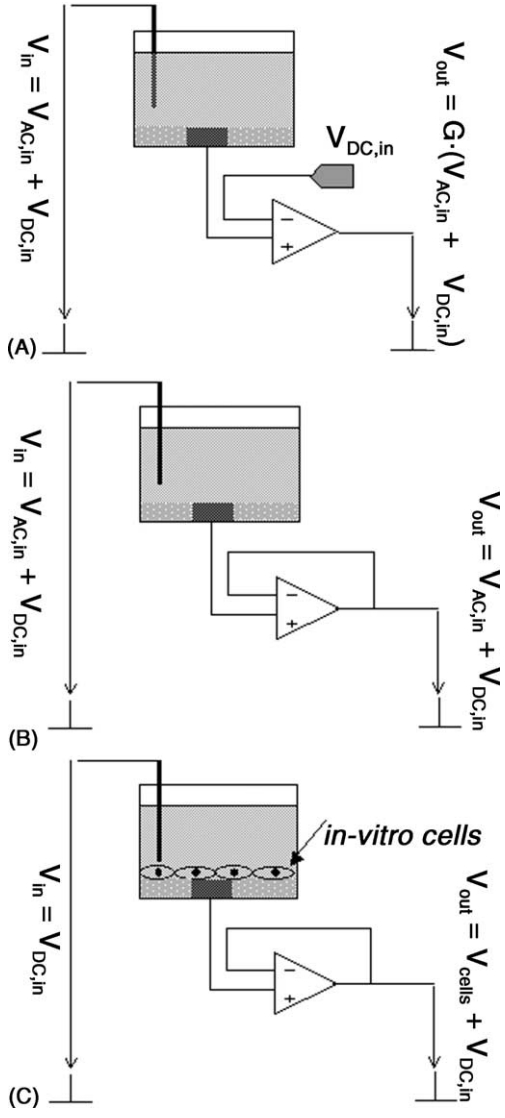

Fig. 3. (A) Open-loop set-up. (B) Closed-loop set-up. (C) Set-up with cell cultures.

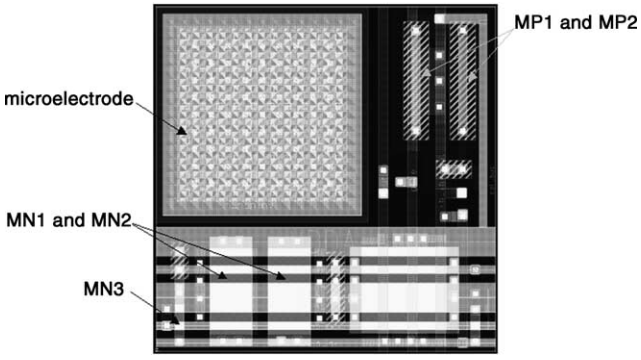

Fig. 4. Single pixel layout.

2.3. Chip post-processing and packaging

The APS–MEAs prototype was fabricated by using a standard 0.5 μm CMOS technology (Alcatel Microelectronics, 5 metal layers technology) with a silicon–aluminium-alloy as the metal layers. This material, due to its rather poor stability in physiological solutions and poor biocompatibility is, however, inadequate for electrophysiological recordings and has to be modified. We have realized this by using an electroless post-processing step that we developed and previously reported (Berdondini et al., 2004). Briefly summarizing the post-processing steps: after receiving the devices from the foundry, the APS–MEAs were cleaned in acetone, rinsed in isopropanol and dried with nitrogen. Then the devices were packaged on a 32 mm × 30 mm printed circuit board (PCB), wire-bonded (Al wires of 50 μm in diameter) and the wires protected with epoxy glue. The gold deposition was performed in two steps at 25 °C by dispensing drops of solutions on the active area. In the first solution (Atomex solution from Engelhard-Clal), gold initiation sites are formed by displacement of aluminium, while in the second solution (Cathagold from Engelhard-Clal, diluted 1:20 with DI water) the actual autocatalytic electroless deposition takes place. For a deposition time of 15 min, the thickness of the gold layer was estimated at about 1 μm.

The post-processing with the electroless deposition is very convenient since it does not require any photolithographic steps, offers a fast deposition rate and moreover, it does not require any inter-layers between the CMOS metal layer and gold. It should be noted that no additional post-processing was performed for modifying the top CMOS standard SiO_2 insulation layer.

A PMMA spacer which also holds a glass culture cylinder (20 mm in diameter and 10 mm in height) was glued onto the PCB using the same epoxy resin (Fig. 5A). The PCB provides a DIP24 socket connector for the rapid mounting and dismounting on the interface board.

2.4. Chip interface board

We built a chip interface for providing the supply voltages (5 $V_{p\text{-}p}$ and 3.3 $V_{p\text{-}p}$) necessary to operate the chip and

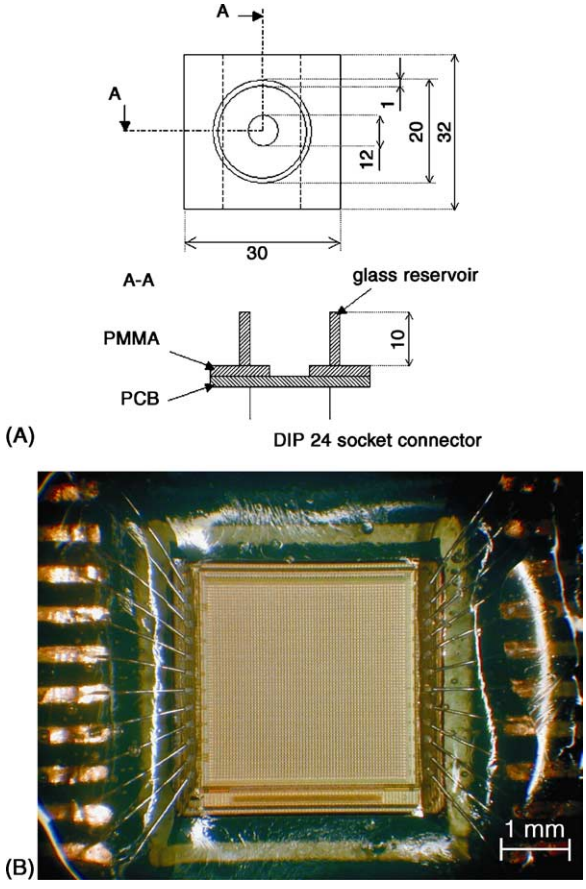

Fig. 5. (A) Chip packaging. (B) Top view of a packaged device.

for evaluating the APS–MEA functionality. The single signal output is connected to an external circuit with different amplification factors: a gain of one used for the open-loop mode and a gain of 100 used for the closed-loop mode. Additionally, in the closed-loop mode, the signal is filtered as shown in Fig. 6A. The on-chip random addressing logic was controlled using a manual switch and providing a six bit address for the column and a six bit address for the row. Currently, this simple interface does not allow rapid switching of the recording electrodes to be performed.

2.5. Electrical characterization in phosphate solution

The functional electrical characterization was performed by applying a small amplitude AC signal ($V_{AC,\,In}$) and a DC polarization signal ($V_{DC,\,In}$) to the platinum wire reference electrode with respect to the electrical ground (Fig. 3A). This wire was connected to an external DC voltage generator (HP E3632A DC Power Supply) in series with the AC signal generator (HP 30120A Waveform Signal Generator). The experiments were performed inside a Faraday cage in a phosphate buffer solution (150 mM, pH adjusted to 7.3 with H_3PO_4). Since the microelectrodes are at a floating potential, no potential drop is established at the microelectrode–electrolyte interface resulting from the DC polarization. In other words,

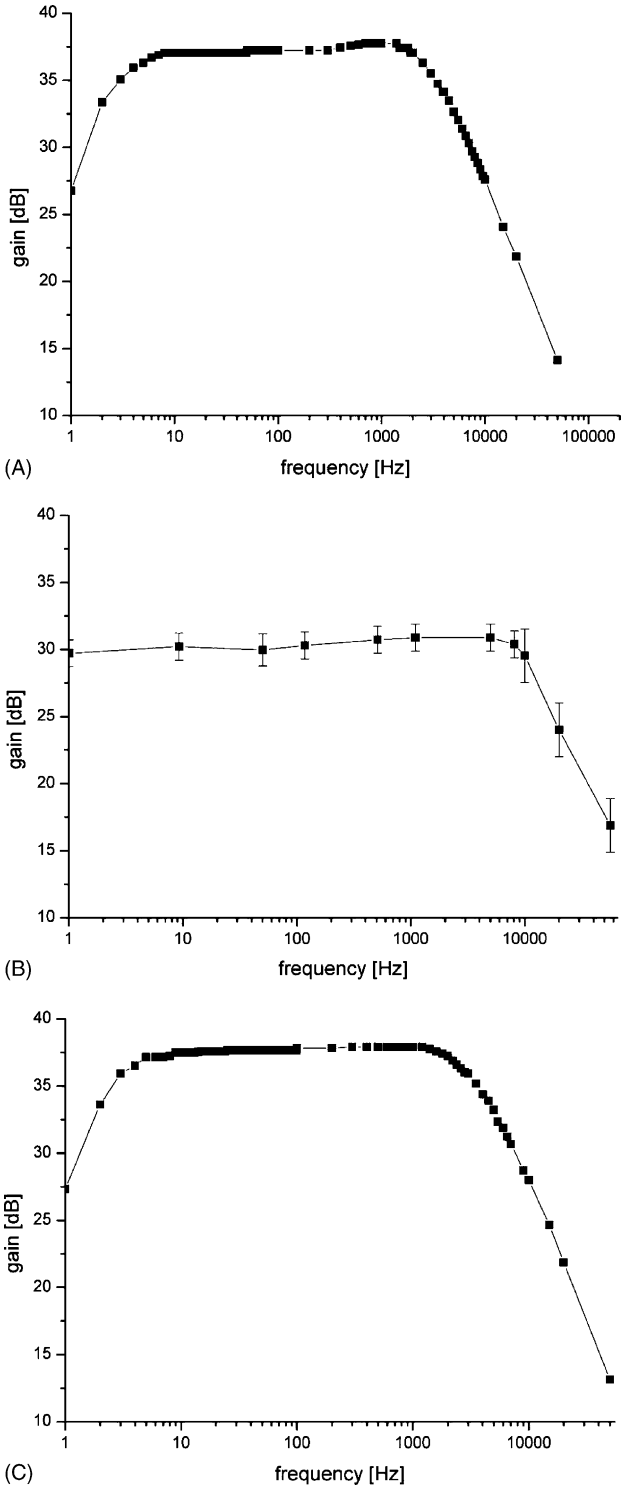

Fig. 6. Gain-frequency behaviour of a single pixel of the APS–MEA in phosphate solution (150 mM). (A) External amplifier gain for the unity-gain mode. (B) Maximal measured open-loop gain of a single pixel pre-amplifier. (C) Behaviour of a single pixel pre-amplifier configured in closed-loop mode and being externally amplified.

the DC polarization does not induce any electrochemical reaction at the microelectrodes.

The gain-frequency behaviour of the amplifier was characterized with a sinusoidal signal with amplitude which was reduced from 100 $mV_{p\text{-}p}$ to 2 $mV_{p\text{-}p}$ using an attenuator (HP 355D VHF Attenuator). The applied frequencies ranged 1–50 kHz. In order to operate the pre-amplifier in open-loop mode, the same DC polarization with respect to the electrical ground must be applied to the input pair, i.e., on the recording microelectrode and on the inverting amplifier input. A potentiometer was used for compensating the DC offset between the inputs. In closed-loop mode (Fig. 3B), the polarization voltage ($V_{DC,\,In}$) and the sinusoidal signal ($V_{AC,\,In}$) were applied only to the platinum wire.

2.6. Cell culture recordings

The devices were rinsed in deionised water, dried with nitrogen, coated with collagen (human placenta, type VI, Sigma) acting as an adhesion promoter and sterilized under UV light for 90 min with the reservoir filled with culture medium. Primary cultures of neonatal rat ventricular cardiomyocytes were obtained using previously published procedures (Rohr et al., 1991). The cell suspension was pre-plated in large culture flasks in order to reduce the fibroblast content and the myocytes remaining in suspension were seeded at a density of 1.9×10^3 cells/mm^2 on the APS–MEAs. The cultures were kept in an incubator at 35 °C in a humidified atmosphere containing 1.2% CO_2, and medium exchanges were performed on the first day after seeding and every other day thereafter with supplemented medium M199 (Gibco, Basel, Switzerland) containing a reduced concentration of serum (5%).

The same set-up described for the electrical characterizations was also used for the electrophysiological tests except that only the DC polarization was applied to the platinum wire (Fig. 3C). The in-pixel amplifier was used in the closed-loop configuration. The output signal of the chip consisted of the polarization voltage ($V_{DC,\,In}$) added to the cellular signal (V_{cells}). The signal was amplified externally and filtered as shown in Fig. 6A and the acquisition was performed by using an oscilloscope (Tektronix, TDS360).

3. Results and discussion

The CMOS chip measures 3.1 mm × 3.4 mm (Fig. 5B) and integrates 64 × 64 pixels, on an active surface of 2.5 mm × 2.5 mm. Each pixel has a dimension of 40 μm × 40 μm, a microelectrode of 20μm × 20 μm and a pre-amplifier. This results in an electrode separation of 20 μm (or 40 μm centre-to-centre). The device has 24 bonding pads; 12 of them are used for digitally addressing the active pixel; 1 is the analogue output and the remaining pads are used for grounding and supply voltages (3.3 V and 5 V).

3.1. In-pixel pre-amplifier simulations

Simulations were used for optimising the pre-amplifier open-loop gain and noise by modifying the channels' length and width of the transistors in the 5-OTA. The dimensions are for transistors MN1 and MN2 of 5 μm in width and 10 μm in length; for transistors MP1 and MP2 of 1 μm in width and 10 μm in length; and for transistors MN3 and MN4 of 1.1 μm in width and 3 μm in length. Once the geometries fixed, the open-loop gain, the bandwidth and the referred input noise were simulated towards transistor geometries and for polarization voltages between 1.4 V and 1.6 V. Gains from 23 dB up to 50 dB with frequency bandwidth of 270 kHz–14 kHz, respectively, were obtained. The polarization voltage allows the programming of the open-loop gain and bandwidth. For both modes, the simulated pre-amplifier referred input noise resulted in 79.6 μV rms.

As previously discussed, a high amplifier input impedance is necessary to compensate the electrode impedance. In the designed circuit, the input impedance is essentially given by the input parasitic capacitance (gate capacitance of the non-inverting input), which is 200 fF. The resulting impedance is then given by $Z_{\text{in}} = 1/2\pi fC$, where f is the frequency. At a frequency of 1.1 kHz, the impedance is 723 MΩ.

3.2. Pre-amplifier characterization in phosphate solution

The in-pixel pre-amplifier of different pixels was characterized in both open and closed-loop modes by manually addressing different pixels. In the open-loop mode, the same DC polarization was applied to the input pair of the pre-amplifier: on the recording microelectrode via the platinum wire and on the inverting input. This potential acted as a reference potential for the measurements in the phosphate solution. The open-loop gain was measured by addressing the recording pixel and application of an AC signal. The maximum gain between 29.5 dB and 30.8 dB over a bandwidth of 10 kHz has been measured for a DC polarization of 0.7 V (Fig. 6B). A similar behaviour, with only small changes in the required polarization voltage for achieving the maximum gain, was observed on all pixels.

The experimental gains and bandwidths are lower than the simulated ones, because of difficulties to stabilize the gain due to the high sensitivity of the differential pair to the noise on the polarization. This noise originates from the difference between the polarization of the two amplifier inputs introduced by the ohmic drop in the solution and at the electrode–electrolyte interfaces. This offset can be compensated, but the polarizations on the two inputs will never be exactly the same and, thus, this will always be a source of noise. Additionally, also the DC signal generator contributes with noise amplified by the open-loop gain of the integrated circuit. The lowest total output noise that we achieved is 500 $\mu V_{p\text{-}p}$, which limits the performances of the open-loop mode.

We can conclude from this first experiment that the contribution of the noise on the input pair has at least three direct consequences for the open-loop mode: it introduces the risk of saturating the amplifier, an additional AC-noise source is added to the output amplified signal, and the stability of the amplifier gain (programmed with the DC polarization) is affected within the bandwidth and versus time. For these reasons, the open-loop mode is not well adapted for our application; although, it shows a useful gain.

The closed-loop mode is easier to operate since the feedback compensates for the instabilities of the polarization. The gain-frequency behaviour of the pre-amplifier in a 150 mM phosphate solution is shown in Fig. 6C. This result confirms a better stability of the pre-amplifier when operated in the unity-gain mode. The measured total noise given by the integrated pre-amplifier, the chip interface and the environmental noise, was of about 80 $\mu V_{p\text{-}p}$.

The results obtained in closed-loop mode from different pixels showed small differences of a few millivolts in the polarization voltages necessary to operate the pre-amplifiers. Such a small mismatch between the pixels can be considered as acceptable but will require an external compensation when operating the device at high addressing frequency. The noise level and the gain-frequency behaviour were equivalent on different pixels.

The simulation of the integrated pre-amplifier noise corresponds to the experimental noise in the closed-loop. This indicates that the main noise source is due to the in-pixel pre-amplifier. Thus, the electroless gold microelectrodes seem to show an excellent noise level due to their roughness and the resulting low impedance. In the open-loop, it was not possible to achieve the same noise level due to the additional, previously discussed, noise sources.

Finally, it is important to note that in both operating modes no cross-talk between the channels was observed when manually switching between the recording pixels. Compared to the passive MEAs where the acquisition is performed in parallel and where the cross-talk is a bigger problem, the APS–MEAs show the advantage of recording sequentially the electrode signals in order to avoid cross-talk.

3.3. Recordings from neonatal rat cardiomyocytes

Electrophysiological measurements were performed by culturing neonatal rat cardiomyocytes on the APS–MEAs. These cultures show a spontaneous electrical activity with high-amplitude (extracellular potentials up to 1–2 $mV_{p\text{-}p}$) and extracellular electrophysiological signals already after two days in vitro.

On all devices the cardiomyocyte monolayers showed synchronous contractile activity with a beat rate of a few hertz (visual observations). This behaviour was identical to cultures raised under standard conditions on glass coverslips and, thus, confirmed the adequate biocompatibility of the APS–MEAs.

Signals from several recording sites were obtained by manually addressing the microelectrodes and data acquisition

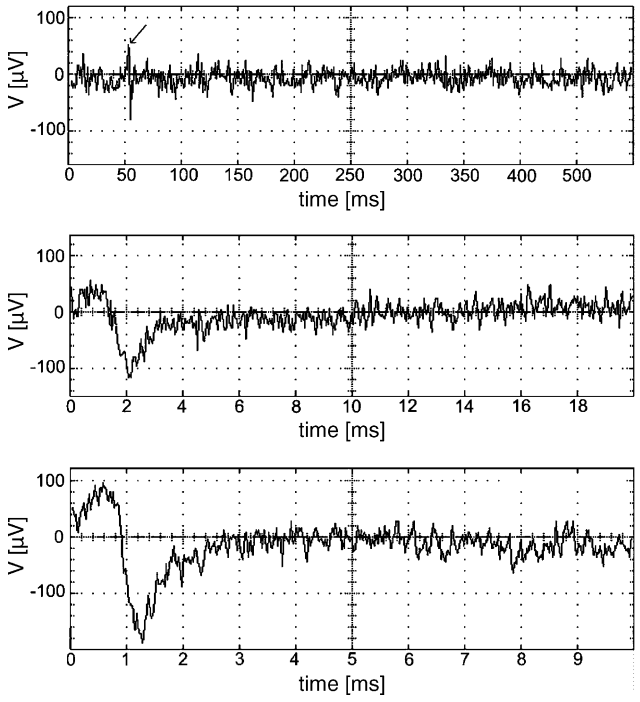

Fig. 7. Single pixel recordings from different pixels and different time scales of spontaneous electrical activity for rat cardiomyocytes cultured on APS–MEAs for 2 days. (A) Sampling rate of 1 kS/s, signal amplitude of 136 $\mu V_{p\text{-}p}$. (B) Sampling rate of 25 kS/s, signal amplitude of 168 $\mu V_{p\text{-}p}$. (C) Sampling rate of 50 kS/s, signal amplitude of 284 $\mu V_{p\text{-}p}$. The shape of the recorded signal is affected by the low sampling rates of the oscilloscope.

was carried out using an oscilloscope (Fig. 7). The oscilloscope does not allow high sampling rates and automatically selects the sampling rate as a function of the time window. For this reason, Fig. 7A–C shows the recorded spontaneous activity from different pixels with different time frames and different sampling frequencies. The recorded spontaneous activity of cardiomyocytes showed signal amplitudes between 130 $\mu V_{p\text{-}p}$ and 300 $\mu V_{p\text{-}p}$ with a total signal length (positive and negative phase) of 2–3 ms. It has to be noted that the signal shapes are affected by the low sampling rates of the oscilloscope. We were able to reuse the APS–MEAs by cleaning the devices with isopropanol and rinsing in DI water.

These results demonstrate that it is possible to record electrophysiological signals. Although the integrated addressing logic could operate at high addressing frequencies, the present set-up did not allow to perform recordings by rapidly switching the pixels. Therefore, it was not possible to experimentally evaluate the switching delay time. Considering that the integrated addressing logic provides a maximum sampling rate of 10 MHz for light-sensitive APS devices and assuming this value for the 64 × 64 pixels APS–MEA this results in a frame rate of 2.44 kHz (or a delay of 0.4 ms) for the whole active area or a frame rate of 20 kHz (or a delay of 50 µs) when reading 500 randomly selected microelectrodes. Thus, the assessment of two-dimensional network activity could be performed over the entire array (low-time resolution) or in specific areas of interest (high-time resolution), by measuring the addressed pixel signal on the single analogue output line of the chip.

4. Conclusions

The aim of this work was to demonstrate the feasibility of the APS concept for realizing high-density microelectrode arrays. Therefore, a first-generation of the APS–MEAs integrating an array of 64 × 64 gold microelectrodes (20 µm × 20 µm), in-pixel pre-amplifiers and on-chip addressing logic on an overall active area of 2.5 mm × 2.5 mm was realized and tested. The APS–MEAs were fabricated by a standard 0.5 µm CMOS process that uses SiO_2 insulation layer and aluminium-alloy electrodes. The electrode material was modified by a post-process gold electroless deposition step.

Electrical tests in a phosphate solution showed that because of a lower noise level, the closed-loop unity-gain mode (80 $\mu V_{p\text{-}p}$) is preferable over the open-loop mode (500 $\mu V_{p\text{-}p}$). In this mode, the device functionality was demonstrated by performing single pixel recordings of spontaneous activity of cultured cardiomyocytes. Electrophysiological signal amplitudes between 130 $\mu V_{p\text{-}p}$ and 300 $\mu V_{p\text{-}p}$ were measured. Both simulation and experimental results obtained demonstrate the functionality of this first-generation of APS–MEA, and constitute, thus, an effective starting point for developing high-resolution devices based on the APS concept.

Although the current noise level is adequate for cardiomyocytes recordings, the next developments will concentrate on reducing the in-pixel pre-amplifier noise for vertebrate neuronal activity recordings. This is an important issue in all extracellular recordings since the electrophysiological signals have amplitudes from 100 $\mu V_{p\text{-}p}$ to 1–2 $mV_{p\text{-}p}$ for rat cardiomyocytes (Kucera et al., 2000) and from 20 $\mu V_{p\text{-}p}$ to 200 $\mu V_{p\text{-}p}$ for vertebrate neurons. The maximum signal bandwidth is between 0 Hz and 4 kHz. The functional characteristics of the pre-amplifier have thus to fulfil the requirements of recording low frequency and small amplitude signals through a high impedance microelectrode–cell–electrolyte interface (mainly capacitive). The current state of the art in analogue amplifier design should allow achieving better signal to noise ratios by further optimisation of the pre-amplifier. Additionally, a high-speed addressing electronics need to be implemented in the recording set-up for rapidly switching the recording pixels. If necessary, the frame rate could be further increased by designing APS–MEAs with additional output signals such as used in high-speed light-sensitive APS devices.

The modular pixel array approach permits the future integration of other pixel functionalities such as stimulation, temperature sensing or pH sensing, in the same pixel or, reducing the electrode pitch, in different pixels. The reduction of the electrode pitch down to cellular or sub-cellular dimensions combined with a large active area introduces new features compared to conventional thin-film MEAs for analysing the

network activity at the cellular or network level. Thus, for example, with respect to signal separation and shape analysis, the high-density MEAs have the advantage of exhibiting a signal redundancy of recordings from neighbouring microelectrodes. By implementing new signal treatment algorithms a better understanding of the cellular network activity can be achieved. This is particularly interesting for the research fields that use in vitro MEAs technology for modelling the signal propagation in cardiomyocyte networks or for studying the behaviour of neuronal networks.

Acknowledgments

The authors thank Ms S. Pochon (IMT, Neuchâtel) for the technical assistance and S. Martinoia (University of Genova, Italy) for the useful discussions. The Office Fédéral de l'Education et de la Science (OFES), Switzerland, is gratefully acknowledged for the financial support.

References

Bai, Q., Wise, K.D., 2001. Single-unit neural recording with active microelectrode arrays. IEEE Trans. Biomed. Eng. 48 (8), 911–920.

Berdondini, L., Overstolz, T., de Rooij, N.F., Koudelka-Hep, M., Martinoia, S., Seitz, P., Wäny, M., Blanc, N., 2002. High resolution electrophysiological activity imaging of in vitro neuronal networks. In: IEEE-EMBS Special Topic Conference in Medicine and Biology, Madison, Wisconsin, USA, pp. 241–244.

Berdondini, L., Overstolz, T., Koudelka-Hep, M., Seitz, P., 2000. High-density microelectrode arrangement. EP1278064.

Berdondini, L., van der Wal, P.D., de Rooij, N.F., Koudelka-Hep, M., 2004. Development of an electroless post-processing technique for depositing gold as electrode material on CMOS devices. Sens. Actuators B-Chem. 99, 505–510.

Bucher, V., Brugger, J., Kern, D., Kim, G.M., Schubert, M., Nisch, W., 2002. Electrical properties of light-addressed sub-μm electrodes fabricated by use of nanostencil-technology. Microelectron. Eng. 61–2, 971–980.

Bucher, V., Brunner, B., Leibrock, C., Schubert, M., Nisch, W., 2001. Electrical properties of a light-addressable microelectrode chip with high electrode density for extracellular stimulation and recording of excitable cells. Biosens. Bioelectron. 16 (3), 205–210.

DeBusschere, B.D., Kovacs, G.T.A., 2001. Portable cell-based biosensor system using integrated CMOS cell-cartridges. Biosens. Bioelectron. 16 (7–8), 543–556.

DeMarse, T.B., Wagenaar, D.A., Blau, A.W., Potter, S.M., 2001. The neurally controlled animat: biological brains acting with simulated bodies. Auton. Rob. 11 (3), 305–310.

Eversmann, B., Jenkner, M., Hofmann, F., Paulus, C., Brederlow, R., Holzapfl, B., Fromherz, P., Merz, M., Brenner, M., Schreiter, M., Gabl, R., Plehnert, K., Steinhauser, M., Eckstein, G., Schmitt-Landsiedel, D., Thewes, R., 2003. A 128 × 128 CMOS biosensor array for extracellular recording of neural activity. IEEE J. Solid-State Circuit 38 (12), 2306–2317.

George, M., Parak, W.J., Gaub, H.E., 2000a. Highly integrated surface potential sensors. Sens. Actuators B-Chem. 69 (3), 266–275.

George, M., Parak, W.J., Gerhardt, I., Moritz, W., Kaesen, F., Geiger, H., Eisele, I., Gaub, H.E., 2000b. Investigation of the spatial resolution of the light-addressable potentiometric sensor. Sens. Actuator A-Phys. 86 (3), 187–196.

Gross, G.W., Williams, A.N., Lucas, J.H., 1982. Recording of spontaneous activity with photoetched microelectrode surfaces from mouse spinal neurones in culture. J. Neurosci. Methods 5, 13–22.

Heer, F., Franks, W., Blau, A., Taschini, S., Ziegler, C., Hirlemann, A., Baltes, H., 2004. CMOS microelectrode array for the monitoring of electrogenic cells. Biosens. Bioelectron. 2004, doi:10.1016/j.bios.2004.02.006.

Heiduschka, P., Romann, I., Ecken, H., Schoning, M., Schuhmann, W., Thanos, S., 2001. Defined adhesion and growth of neurones on artificial structured substrates. Electrochim. Acta 47 (1–2), 299–307.

Jimbo, Y., Tateno, T., Robinson, H.P.C., 1999. Simultaneous induction of pathway-specific potentiation and depression in networks of cortical neurons. Biophys. J. 76 (2), 670–678.

Keefer, E.W., Gramowski, A., Stenger, D.A., Pancrazio, J.J., Gross, G.W., 2001. Characterization of acute neurotoxic effects of trimethylolpropane phosphate via neuronal network biosensors. Biosens. Bioelectron. 16 (7–8), 513–525.

Kucera, J.P., Heuschkel, M.O., Renaud, P., Rohr, S., 2000. Power-law behavior of beat-rate variability in monolayer cultures of neonatal rat ventricular myocytes. Circ. Res. 86 (11), 1140–1145.

Lehmann, M., Baumann, W., Brischwein, M., Gahle, H.J., Freund, I., Ehret, R., Drechsler, S., Palzer, H., Kleintges, M., Sieben, U., Wolf, B., 2001. Simultaneous measurement of cellular respiration and acidification with a single CMOS ISFET. Biosens. Bioelectron. 16 (3), 195–203.

Maher, M.P., Pine, J., Wright, J., Tai, Y.C., 1999. The neurochip: a new multielectrode device for stimulating and recording from cultured neurons. J. Neurosci. Methods 87 (1), 45–56.

Martinoia, S., Bove, M., Tedesco, M., Margesin, B., Grattarola, M., 1999. A simple microfluidic system for patterning populations of neurons on silicon micromachined substrates. J. Neurosci. Methods 87 (1), 35–44.

Morefield, S.I., Keefer, E.W., Chapman, K.D., Gross, G.W., 2000. Drug evaluations using neuronal networks cultured on microelectrode arrays. Biosens. Bioelectron. 15 (7–8), 383–396.

Mussa-Ivaldi, F.A., Miller, L.E., 2003. Brain-machine interfaces: computational demands and clinical needs meet basic neuroscience. Trends Neurosci. 26 (6), 329–334.

Najafi, K., Wise, K.D., 1986. An implantable multielectrode array with on-chip signal processing. J. Solid-State Circuits sc-21 (6), 1035–1044.

Offenhäusser, A., Knoll, W., 2001. Cell-transistor hybrid systems and their potential applications. Trends Biotechnol. 19 (2), 62–66.

Pancrazio, J.J., Bey, P.P., Loloee, A., Manne, S.R., Chao, H.C., Howard, L.L., Gosney, W.M., Borkholder, D.A., Kovacs, G.T.A., Manos, P., Cuttino, D.S., Stenger, D.A., 1998. Description and demonstration of a CMOS amplifier-based-system with measurement and stimulation capability for bioelectrical signal transduction. Biosens. Bioelectron. 13 (9), 971–979.

Pine, J., 1980. Recording action-potentials from cultured neurons with extracellular micro-circuit electrodes. J. Neurosci. Methods 2 (1), 19–31.

Rohr, S., Schölly, D.M., Kleber, A.G., 1991. Patterned growth of neonatal rat heart cells in culture Morphological and electrophysiological characterization. Circ. Res. 68, 114–130.

Saneinejad, S., Shoichet, M.S., 2000. Patterned poly(chlorotrifluoroethylene) guides primary nerve cell adhesion and neurite outgrowth. J. Biomed. Mater. Res. 50 (4), 465–474.

Shahaf, G., Marom, S., 2001. Learning in networks of cortical neurons. J. Neurosci. 21 (22), 8782–8788.

Willemin, M., Blanc, N., Lang, G.K., Lauxtermann, S., Schwider, P., Seitz, P., Wany, M., 2001. Optical characterization methods for solid-state image sensors. Opt. Lasers Eng. 36 (2), 185–194.

Yeung, C.K., Lauer, L., Offenhäusser, A., Knoll, W., 2001. Modulation of the growth and guidance of rat brain stem neurons using patterned extracellular matrix proteins. Neurosci. Lett. 301, 147–150.